Original Article

Near-infrared temperature-switchable fluorescence nanoparticles

Shuai Yu[1,2], Zhen Wang[1,2], Tingfeng Yao[1,2], Baohong Yuan[1,2]

[1]Ultrasound and Optical Imaging Laboratory, Department of Bioengineering, The University of Texas at Arlington, Arlington, TX 76019, USA; [2]Joint Biomedical Engineering Program, The University of Texas at Arlington and The University of Texas Southwestern Medical Center at Dallas, TX 75390, USA

Correspondence to: Baohong Yuan. Department of Bioengineering, 500 UTA Blvd, Arlington, TX 76010, USA. Email: baohong@uta.edu.

Background: Near infrared (NIR) environment-sensitive fluorophores are highly desired for many biomedical applications because of its non-invasive operation, high sensitivity and specificity, non-ionizing radiation and deep penetration in biological tissue. When the fluorophores are appropriately encapsulated in or conjugated with some thermal-sensitive polymers, they could work as excellent temperature-sensing probes.

Methods: In this study, we synthesized and characterized a series of NIR temperature-switchable nanoparticles based on two series of NIR fluorophores aza-BODIPY (ADP is used for abbreviation in this work) and Zinc phthalocyanine (ZnPc) and four pluronic polymers (F127, F98, F68 and F38). Encapsulating the fluorophores in the polymers by sonication, we synthesized the nanoparticles that showed switch-like functions of the fluorescence intensity (and/or lifetime) as the temperature, with high switch on-to-off ratio. We also investigated various factors that might change the temperature thresholds (T_{th}) of the switch functions, in order to control T_{th} during synthesis.

Results: These nanoparticles showed excellent temperature-switchable properties of fluorescence intensity and/or lifetime. Meanwhile, some factors (i.e., pluronic categories and nanoparticles' concentration) significantly affected the nanoparticles' T_{th}s while other (i.e., fluorophore categories) that weakly affected T_{th}s.

Conclusions: By selecting appropriate pluronic categories and adjusting the nanoparticle's concentration, we can synthesize the nanoparticles with a wide range of T_{th}s. These temperature-switchable fluorescence nanoparticles can be used for biomedical imaging and *in vivo* tissue temperature sensing/imaging.

Keywords: Near infrared temperature-switchable fluorescence; imaging and sensing; pluronic nanoparticles; Aza-BODIPY and Zinc phthalocyanine fluorophores

Submitted Jun 25, 2020. Accepted for publication Aug 25, 2020.
doi: 10.21037/qims-20-797
View this article at: http://dx.doi.org/10.21037/qims-20-797

Introduction

Near infrared (NIR) fluorescence imaging and sensing has been attracting much attention in biomedical applications during the past decades due to its non-invasive operation, high sensitivity and specificity, non-ionizing radiation as well as deep penetration in biological tissue (1). In comparison to other imaging techniques, such as ultrasound, X-ray, magnetic resonance imaging (MRI), and positron-emission tomography (PET), fluorescence imaging provides benefits such as low cost, bio-safety, and fast detection. Also, fluorescence imaging is capable of multicolor imaging and thus it could track many interesting cellular and/or molecular-level biological interactions (2).

Recently, switchable fluorescence probes (SFPs) have gained great interest for detecting specific environmental changes in biological tissue. They have high sensitivity and specificity to a certain stimulus (3-5). A SFP usually stays at an "off" state so its fluorescence is weak. When a stimulus is applied, it can be switched "on" to emit strong

fluorescence. The types of the stimulus can be physical (such as temperature), chemical (such as pH) or biological (such as biomolecule interaction) (4). Among various SFPs, one of them is the temperature-switchable fluorescence probe (T-SFP) (6-12). When a polarity- and viscosity-sensitive fluorophore is encapsulated in temperature-sensitive polymers, the fluorescence could become temperature-sensitive. This is because when the temperature rises over the lower critical solution temperature (LCST) of the polymers, the polymers experience a phase transition from hydrophilic to hydrophobic. Thus, the encapsulated fluorophores experience a microenvironment change from water-rich to polymer-rich and therefore a change of the polarity and/or viscosity of the microenvironment. This change can significantly increase the quantum yield of the polarity- and viscosity-sensitive fluorophore. As a result, when a T-SFP stays in a temperature below the LCST, its fluorescence is usually weak. When temperature rises over the LCST, the T-SFP can emit strong fluorescence.

In our previous works (6), we summarized five parameters that characterize the performance of a T-SFP. They are: (I) the fluorescence peak excitation and emission wavelengths (λ_{ex} and λ_{em}); (II) the fluorescence intensity ratio between its on and off states (I_{on}/I_{off}); (III) the fluorescence lifetime ratio between its on and off states (τ_{on}/τ_{off}); (IV) the temperature threshold to switch on the fluorescence (T_{th}); and (V) the temperature transition bandwidth (T_{BW}). In this work, we synthesized, characterized, and selected a series of T-SFPs. We adopted two series of NIR fluorophores aza-BODIPY (ADP, we will use ADP for abbreviation in this work) and Zinc phthalocyanine (ZnPc) and four pluronic polymers. Each of fluorophore was encapsulated in one type of pluronic polymer to form temperature-switchable nanoparticles by sonication. The dyes in the ADP and ZnPc families are excellent NIR fluorophores and their quantum efficiencies vary in response to solvents' polarity and viscosity change (8,9,13,14). The pluronic polymers (i.e., F127, F98, F68, and F38) contain two hydrophilic poly(ethylene oxide) (PEO) and one hydrophobic poly(propylene oxide) (PPO), and they are arranged in a PEO-PPO-PEO triblock structure. When the polymers form nanoparticles, the dye molecules may be more likely encapsulated inside the particles by the hydrophobic part. When the temperature is increased above a threshold, the particle structure may be changed significantly, which makes the dye environment more hydrophobic, less polar and more viscous. Thus, the polarity- and/or viscosity-sensitive dyes experience an increase of the quantum efficiency and the fluorescence emission intensity. By combination of the two series of dyes and the four polymers, we can select the nanoparticles with excellent temperature-switchable fluorescence properties.

We characterized these nanoparticles based on the above mentioned parameters. We also investigated several factors that might change their T_{th}s. These nanoparticles can be potentially used for fluorescence imaging and sensing (15-25). This work has several novelties (1). This work adopted four pluronic polymers (F127, F98, F68, and F38). The four polymers have different lower critical solution temperatures (LCSTs) and thus provide a wide dynamic range of T_{th} (2). This work recognized two factors that could significantly affect the nanoparticle's T_{th}s: one is pluronic categories as mentioned in (I), and another is nanoparticles' concentration. The nanoparticles' concentration will affect their T_{th}s significantly. Base on (I) and (II), we can synthesize the nanoparticles with a wide range and a precise control of T_{th}s, and this is very useful when they are adopted for temperature sensing/imaging (IV). This work adopted two series of NIR dyes (ADP and ZnPC) for the synthesis and provide different spectral fingerprints for multi-color fluorescence imaging.

Methods

Chemical materials

The ADP fluorophores include BF2-chelated azadipyrromethene (i.e., aza-BODIPY, ADP is used in this study for short. As a note, in the following paragraphs, when we refer ADP as a specific dye, it means azaBODIPY without any additional functional group unlike other three types do.), BF2-chelated 4-{2-[3-(4-hydroxyphenyl)-5-phenyl-1H-pyrrol-2ylimino]-5-phenyl-2H-pyrrol-3-yl}phenol ($ADP(OH)_2$-Top), BF2-chelated [5-(4-hydroxyphenyl)-3-phenyl-1H-pyrrol-2-yl]-[5-(4-hydroxyphenyl)-3-phenylpyrrol-2-ylidene] amine ($ADP(OH)_2$-Bottom), BF2-chelated azadipyrromethene with two cyanocinnamic acid groups ($ADP(CA)_2$). They were synthesized at the Department of Chemistry, University of North Texas (Denton). The details of aza-BODIPY fluorophores can be found in our previous works (8,9,26-28). The ZnPc fluorophores include zinc phthalocyanine (ZnPc), zinc 2, 9, 16, 23-tetra-tert-butyl-29H, 31H-phthalocyanine (ZnttbPc), and zinc 1, 2, 3, 4, 8, 9, 10, 11, 15, 16, 17, 18, 22, 23, 24, 25-hexadecafluoro-29H, 31H-phthalocyanine (ZnHFPc). They were purchased

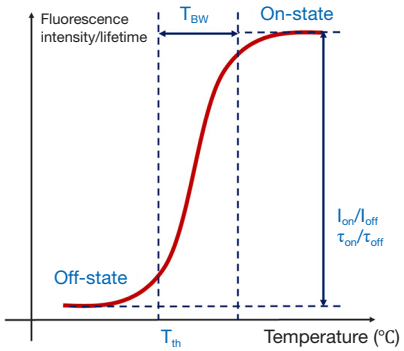

Figure 1 Characterization of fluorescence intensity or lifetime as a function of temperature. I_{on}/I_{off}: the fluorescence intensity ratio between its on- and off-states; τ_{on}/τ_{off}: the fluorescence lifetime ratio between its on- and off-states; T_{th}: the temperature threshold to switch on the fluorescence; T_{BW}: the temperature transition bandwidth.

from Sigma-Aldrich Corporate (St. Louis, MO, USA). The details of ZnPc related fluorophores can be found in manufacturer's datasheet (29). The polymers include pluronics F127, F98, F68, and F38. Tetrabutylammonium iodide (TBAI), pluronic F127, and chloroform was purchased from Sigma-Aldrich Corporate (St. Louis, MO, USA). Pluronic F98, F68, F38 were purchased from BASF Corporation (Vandalia, IL, USA). All chemicals were used as received without further purification.

Synthesis of ADP/ZnPC encapsulated pluronic nanoparticles

The synthesis protocol is from our previous work (8,9). 5 g (or 1 g) pluronic polymer (F127, F98, F68, or F38) was dissolved in 100 mL DI water (pH=8.5) to make 5% (or 1%) pluronic solution. Each of ADP-series fluorophores (ADP, $ADP(OH)_2$-Bottom, $ADP(OH)_2$-Top, or $ADP(CA)_2$) or ZnPc-series fluorophores (ZnPc, ZnttbPc, or ZnHFPc) was selected and encapsulated in the nanoparticles. 0.4 mg ADP fluorophore (or 1.2 mg ZnPc fluorophore) was mixed with 4.8 mg TBAI (cosolvent) and then dissolved in 6 mL chloroform. The fluorophore solution was added dropwise to 15 mL of the pluronic solution, with 600 rpm stirring. The mixture was then under sonication (power =40 Watts) for 4 mins to form fluorophore-encapsulated pluronic-based nanoparticles. The mixture was stirred at 475 rpm in chemical hood overnight until chloroform evaporated thoroughly. The solution was filtered (filter pole size: 450 μm) to purify the sample. All steps were conducted at room temperature. The synthesis protocols are the same for all polymers' and dyes' combination.

Fluorescence intensity and lifetime measurement system

The measurement system was developed in our previous work (6). Briefly, the excitation light was from a sub-nanosecond nitrogen-pumped pulsed dye-laser with wavelength centered at 655 nm and pulse width ~0.8 ns. One band-pass interference excitation filter (650/60 nm) was placed in front of the laser output. The nanoparticle sample (volume =3 mL) was placed in a quartz cuvette and submerged in a transparent glass tank filled with water. The water temperature was controlled via a temperature controller. The laser beam illuminated the sample in the cuvette and the emitted fluorescence photons were captured by a photomultiplier tube (PMT) at a 90-degree angle from the laser beam. One band-pass interference emission filter (711/25 nm) was placed in front of the PMT. Finally, the signal was acquired in a multichannel oscilloscope. The fluorescence pulses were recorded at different temperatures. The excitation laser pulse was also measured. We adopted the measured laser pulse as an impulse response function (IRF) of the system. At each temperature, we counted the signal pulse peak as fluorescence intensity. In order to calculate fluorescence lifetime, we de-convolved the normalized fluorescence pulse from IRF and got an exponential decay function. We counted the decay constant as fluorescence lifetime. It is worth mentioning that we measured all the samples' fluorescence response to a temperature change through conventional heating (i.e., water bath) rather than ultrasound-induced heating, because the purpose of this study is to quantify the thermal properties of these agents.

Characterization of thermal switchable properties of fluorescence from the nanoparticles

As mentioned in the *Introduction*, there are five parameters that can be used to quantify the thermal switchable properties of the fluorescence from the nanoparticles. *Figure 1* shows a diagram indicating some of the characterization parameters. In the plot, the x-axis represents the environment temperature of the nanoparticle, and the y-axis represents the nanoparticle's fluorescence intensity (or lifetime). The fluorescence intensity (or lifetime) changes as a function of temperature. Typically, the

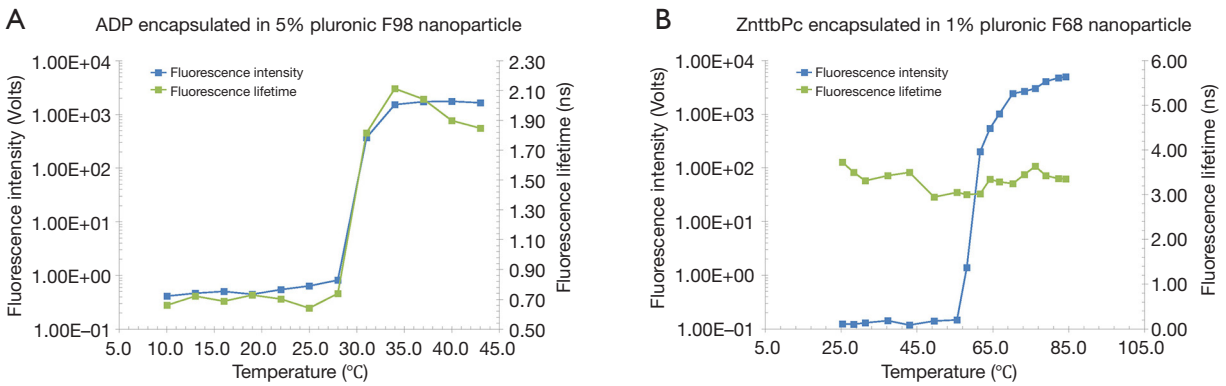

Figure 2 Fluorescence intensity and lifetime as a function of temperature of (A) ADP encapsulated in 5% pluronic F98 nanoparticle; and (B) ZnttbPc encapsulated in 1% pluronic F68 nanoparticle.

fluorescence intensity (or lifetime) is weak (or short) when the temperature is below the T_{th}. When the temperature rises above the T_{th}, the fluorescence intensity (or lifetime) increases significantly. When the temperature rises across the TBW, the fluorescence intensity (or lifetime) becomes stabilized again. The fluorescence intensity (or lifetime) ratio between the on and off states are termed as Ion/Ioff (or τ_{on}/τ_{off}). For temperature imaging/sensing, an ideal T-SFP should have (I) NIR λ_{ex} and λ_{em} (which are mainly determined by the fluorophore); (II) high I_{on}/I_{off} and τ_{on}/τ_{off}; and (III) adjustable T_{th} and TBW. NIR wavelengths provide good penetration to biological tissue; high I_{on}/I_{off} and τ_{on}/τ_{off} provide high temperature sensitivity; and adjustable T_{th} and TBW provide an appropriate range of temperature imaging/sensing. Although the reversibility of these nanoparticles is not measured in this work, our previous works based on some nanoparticles used in this study have shown that the nanoparticles can be switched on and off repeatedly for several cycles (8,20).

One of the motivations of this work is to evaluate these nanoparticles with different combination of dyes and polymers and select those with excellent temperature-switchable fluorescence property. The characterizations of nanoparticles could be found in our previous work (8,15). In addition, we evaluate the encapsulation efficiency of each nanoparticle based on the its temperature-fluorescence property due to the fact that it is difficult to accurately measure encapsulation efficiency by directly measuring the percentage of dye precipitates (i.e., free dyes outside encapsulation). Those nanoparticles with excellent temperature switchable fluorescence property can be selected for future uses, such as USF imaging, temperature measurement, and other applications.

Results

Fluorescence intensity and lifetime vs. temperature

As described in the *Methods*, we measured the nanoparticles' fluorescence intensity and lifetime as a function of temperature and characterized the measurement results. *Figure 2* shows two examples. In *Figure 2A*, it shows the measurement of ADP encapsulated in 5% pluronic F98 nanoparticle. It has a high I_{on}/I_{off} =~1,845, and a high τ_{on}/τ_{off} =2.86 (τ_{on} =2.11 ns), which means both its fluorescence intensity and lifetime increase significantly when the temperature rises over its T_{th}. Its T_{th} =~28 ℃, and Tbw =~6 ℃. *Figure 2B* show the measurement of ZnttbPc in 1% pluronic F68 nanoparticle. Similarly, it also has a high I_{on}/I_{off} =~16,395. Differently, its fluorescence lifetime slightly changes with a temperature rise. Its τ_{on}/τ_{off} =1.06 (τ_{on} =3.25 ns). Its T_{th} =~56 ℃, and Tbw =~15 ℃. Based on these two examples, we found their I_{on}/I_{off}, Tth, τ_{on}/τ_{off}, and Tbw varied. Their characterizations were also presented in *Table 1*. In this work, we synthesized all the nanoparticles based on different combinations of fluorophore categories and pluronic categories as well as pluronic concentrations. Then, we characterized and selected these nanoparticles based on their thermos-switchable properties of fluorescence, from three perspectives: (I) those with a high I_{on}/I_{off}; (II) those with a high τ_{on}/τ_{off}; and (III) those with various T_{th}s. Note that some nanoparticles didn't show a thermal-switchable property (i.e., a low I_{on}/I_{off} and/or τ_{on}/τ_{off}) and were excluded. After selection, we studied several factors that affected the nanoparticles' T_{th}s. The results were presented and

Table 1 Examples of nanoparticle's temperature-switchable fluorescence characterization

	I_{on}/I_{off}	T_{th} (℃)	τ_{on}/τ_{off}, τ_{on} (ns)	T_{bw} (℃)
ADP in 5% F98 nanoparticle	1845	28	2.86, 2.11	6
ZnttbPc in 1% F68 nanoparticle	16395	56	1.06, 3.25	15

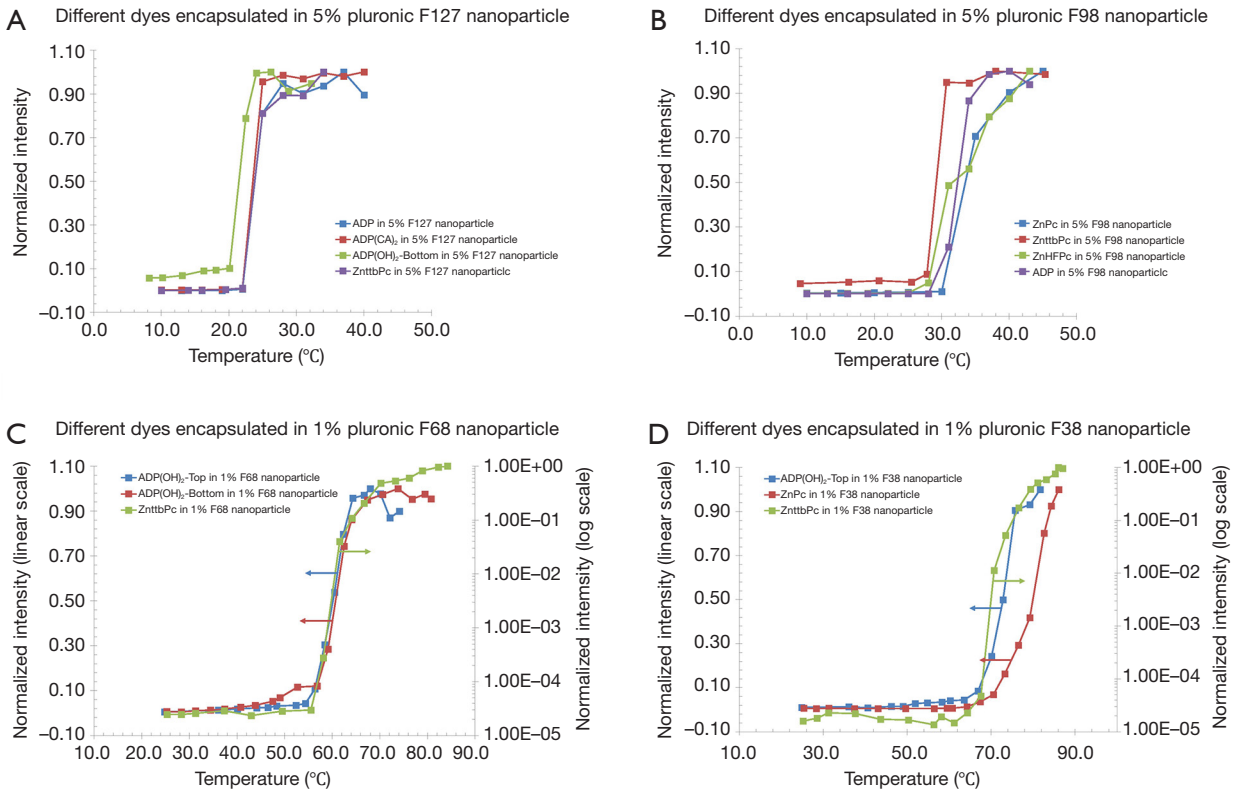

Figure 3 Fluorescence intensity as a function of temperature of (A) ADP, $ADP(CA)_2$, $ADP(OH)_2$-Bottom, and ZnttbPc encapsulated in 5% pluronic F127 nanoparticle; (B) ZnPc, ZnttbPc, ZnHFPc, and ADP encapsulated in 5% pluronic F98 nanoparticle; (C) $ADP(OH)_2$-Top, $ADP(OH)_2$-Bottom, and ZnttbPc encapsulated in 1% pluronic F68 nanoparticle; and (D) ADP(OH)2-Top, ZnPc, and ZnttbPc encapsulated in 1% pluronic F38 nanoparticle.

discussed in the next sections.

Temperature threshold vs. fluorophores

In this section, we studied the variation of T_{th}s. Four polymer solutions were prepared based on different types of pluronics and concentrations: (I) 5% F127; (II) 5% F98; (III) 1% F68; and (IV) 1% F38. In each polymer solution, different fluorophores were encapsulated and the nanoparticles were synthesized and characterized. In 5% F127 nanoparticle, four fluorophores [i.e., ADP, $ADP(CA)_2$, $ADP(OH)_2$-Bottom, and ZnttbPc] were encapsulated. *Figure 3A* shows their normalized fluorescence intensity as a function of temperature. Their T_{th}s were ~22, 22, 20, and 22 ℃, respectively. It shows their T_{th}s were very close to each other (~2 ℃ difference). Likewise, *Figure 3B* shows the normalized fluorescence intensity as a function of temperature of four samples: ADP in 5% F98 nanoparticle, ZnPc in 5% F98 nanoparticle, ZnttbPc in 5% F98 nanoparticle, and ZnHFPc in 5% F98 nanoparticle. Their T_{th}s were ~28, 30, 28, and 25 ℃, respectively. Also, their T_{th}s were close to each other (≤5 ℃). Similar results were

Table 2 Temperature-switchable fluorescence characterization: fluorophore types weakly affected T_{th}s

	I_{on}/I_{off}	T_{th} (℃)	τ_{on}/τ_{off}, τ_{on} (ns)	T_{bw} (℃)
ADP in 5% F127 nanoparticle	159	22	2.67, 2.69	6
$ADP(CA)_2$ in 5% F127 nanoparticle	100	22	1.44, 1.25	3
$ADP(OH)_2$-Top in 5% F127 nanoparticle	10	20	1.14, 1.52	4
ZnttbPc in 5% F127 nanoparticle	69	22	9.69, 2.64	3
ADP in 5% F98 nanoparticle	1845	28	2.86, 2.11	6
ZnPc in 5% F98 nanoparticle	67	30	2.17, 2.44	5
ZnttbPc in 5% F98 nanoparticle	941	28	10.79, 2.55	3
ZnHFPc in 5% F98 nanoparticle	166	25	12.50, 1.61	9
$ADP(OH)_2$-Top in 1% F68 nanoparticle	22	54	1.48, 0.32	10
$ADP(OH)_2$-Bottom in 1% F68 nanoparticle	8	57	1.26, 1.38	11
ZnttbPc in 1% F68 nanoparticle	16395	56	1.06, 3.25	15
$ADP(OH)_2$-Top in 1% F38 nanoparticle	20	64	1.29, 0.26	12
ZnPc in 1% F38 nanoparticle	56	64	0.87, 3.17	18
ZnttbPc in 1% F38 nanoparticle	16887	64	0.92, 3.31	15

also presented when different dyes were encapsulated in 1% F68 nanoparticles (*Figure 3C*) or 1% F38 nanoparticles (*Figure 3D*). The T_{th}s were close to each other (≤5 ℃) when the nanoparticles had the same type of pluronic and the same concentration. All the nanoparticles showed excellent thermal-switchable properties of fluorescence (high I_{on}/I_{off} and/or τ_{on}/τ_{off}). Their characterization results were summarized in *Table 2*. In this section, we concluded that the fluorophore type weakly affected the nancapsules' T_{th}s (T_{th} difference ≤2–5 ℃), when nanoparticles were synthesized based on the same type of pluronic and concentration.

Temperature threshold vs. pluronic types

Figure 3 also indicated that the nanoparticles' T_{th}s varied significantly when using different types of pluronics. In this section, we studied this effect in details. We encapsulated the same fluorophore in nanoparticles using different pluronics. The nanoparticles were characterized and compared with each other. *Figure 4A* shows the characterization results of four samples: $ADP(OH)_2$-Top in 1% F127 nanoparticle, $ADP(OH)_2$-Top in 1% F98 nanoparticle, $ADP(OH)_2$-Top in 1% F68 nanoparticle, $ADP(OH)_2$-Top in 1% F38 nanoparticle. Based on the normalized fluorescence intensities as a function of temperature, their T_{th}s were ~24, 34, 54, and 64 ℃, respectively. Since the same fluorophore (i.e., $ADP(OH)_2$-Top) and pluronic concentration were adopted, the major factor that leaded to the change of the nanoparticles' T_{th}s is the types of the pluronics. *Figure 4B,C,D* shows the similar results when other fluorophores were used (i.e., ZnttbPc in *Figure 4B*, ADP in *Figure 4C*, and ZnPc in *Figure 4D*). All the nanoparticles in *Figure 4* show excellent thermal-switchable properties and their characterization results were summarized in *Table 3*. These examples indicate that the T_{th}s were significantly affected by the types of pluronics. It is worth mentioning that, in these plots, some curves were presented in different scales (linear or log scale) for a better visualization, due to that the nanoparticles' I_{on}/I_{off}s varied significantly in scale (from tens to ten thousands of folds). Based on the results in *Figure 4*, we conclude that the type of pluronics is a main factor that significantly changes the T_{th}s of nanoparticles. Briefly, F127-based nanoparticle provided the lowest T_{th} and F38-based nanoparticle provided the highest. The pluronics' T_{th} sequence is F127 < F98 < F68 < F38. This is because that the T_{th}s of nanoparticles were mainly related to the LCSTs of the pluronics.

Temperature threshold vs. nanoparticle concentrations

In this section, we studied another factor: the concentrations of the nanoparticles, which also affected the T_{th}s. The

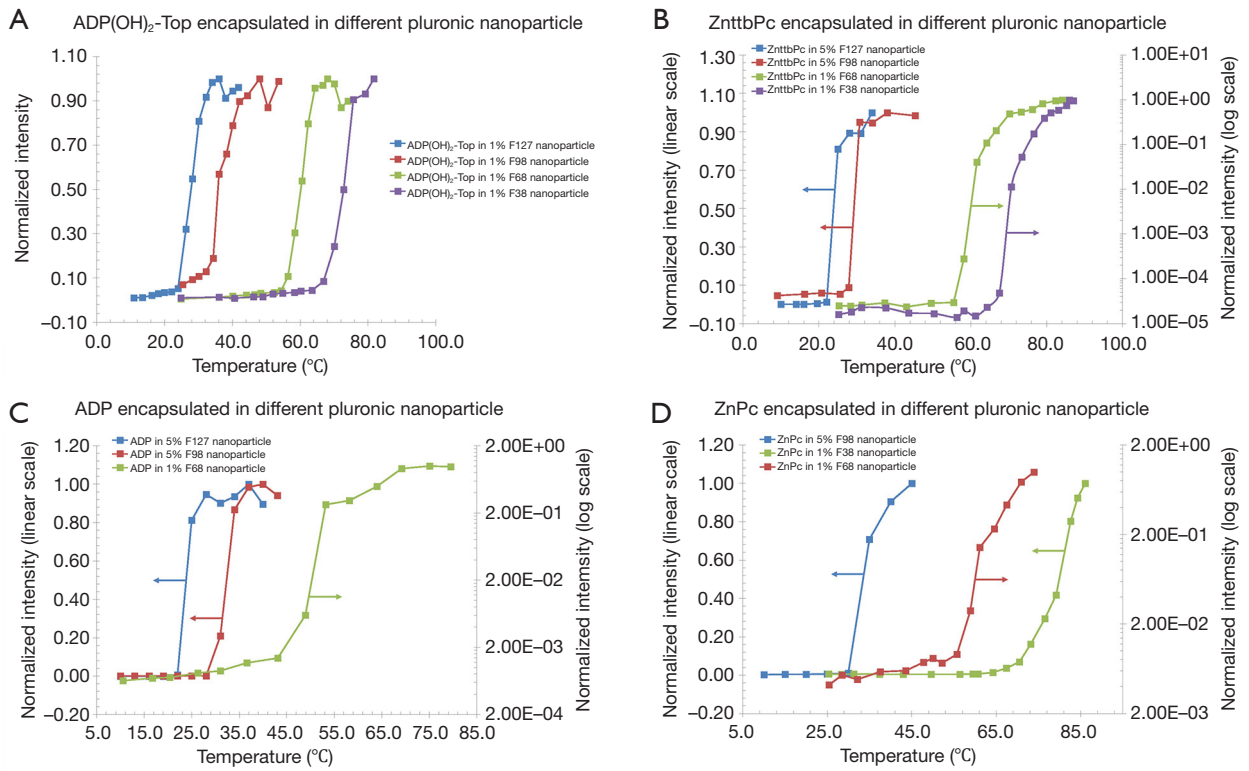

Figure 4 Fluorescence intensity as a function of temperature of (A) $ADP(OH)_2$-Top encapsulated in 1% pluronic F127, 1% pluronic F98, 1% pluronic F68, and 1% pluronic F38 nanoparticle; (B) ZnttbPc encapsulated in 5% pluronic F127, 5% pluronic F98, 1% pluronic F68, and 1% pluronic F38 nanoparticle; (C) ADP encapsulated in 5% pluronic F127, 5% pluronic F98, and 1% pluronic F68 nanoparticle; and (D) ZnPc encapsulated in 5% pluronic F98, 1% pluronic F68, and 1% pluronic F38 nanoparticle.

Table 3 Temperature-switchable fluorescence characterization: pluronic types significantly affected T_{th}s

	I_{on}/I_{off}	T_{th} (℃)	τ_{on}/τ_{off}, τ_{on} (ns)	T_{bw} (℃)
$ADP(OH)_2$-Top in 1% F127 nanoparticle	17	24	1.03, 0.30	8
$ADP(OH)_2$-Top in 1% F98 nanoparticle	8	34	2.34, 0.77	8
$ADP(OH)_2$-Top in 1% F68 nanoparticle	22	54	1.48, 0.32	10
$ADP(OH)_2$-Top in 1% F38 nanoparticle	20	64	1.29, 0.26	12
ZnttbPc in 5% F127 nanoparticle	69	22	9.69, 2.64	3
ZnttbPc in 5% F98 nanoparticle	941	28	10.79, 2.55	3
ZnttbPc in 1% F68 nanoparticle	16,395	56	1.06, 3.25	15
ZnttbPc in 1% F38 nanoparticle	16,887	64	0.92, 3.31	15
ADP in 5% F127 nanoparticle	159	22	2.67, 2.69	6
ADP in 5% F98 nanoparticle	1,845	28	2.86, 2.11	6
ADP in 1% F68 nanoparticle	152	49	1.85, 0.71	20
ZnPc in 5% F98 nanoparticle	67	30	2.17, 2.44	5
ZnPc in 1% F68 nanoparticle	16	56	0.93, 2.37	5
ZnPc in 1% F38 nanoparticle	56	64	0.87, 3.17	18

Table 4 Temperature-switchable fluorescence characterization: T_{th} increased with the decrease of nanoparticle concentration

	I_{on}/I_{off}	T_{th} (℃)	τ_{on}/τ_{off}, τ_{on} (ns)	T_{bw} (℃)
$ADP(OH)_2$-Bottom in 5% F98 nanoparticle	9	28	1.29, 1.58	8
$ADP(OH)_2$-Bottom in 1% F98 nanoparticle	84	34	1.18, 1.52	6
$ADP(OH)_2$-Bottom in 0.2% F98 nanoparticle	40	37	1.21, 1.55	7
$ADP(OH)_2$-Bottom in 0.04% F98 nanoparticle	29	41	1.02, 1.31	10
$ADP(OH)_2$-Bottom in 5% F127 nanoparticle	10	20	1.14, 1.52	4
$ADP(OH)_2$-Bottom in 1% F127 nanoparticle	5	24	1.19, 1.77	4
$ADP(OH)_2$-Bottom in 0.2% F127 nanoparticle	6	26	1.24, 1.75	4
$ADP(OH)_2$-Bottom in 0.04% F127 nanoparticle	3	30	1.06, 1.85	6
$ADP(OH)_2$-Top in 5% F68 nanoparticle	7	48	1.30, 1.03	6
$ADP(OH)_2$-Top in 1% F68 nanoparticle	14	53	1.74, 0.43	8
ZnttbPc in 5% F98 nanoparticle	941	28	10.79, 2.55	3
ZnttbPc in 1% F98 nanoparticle	876	33	12.21, 2.50	5

nanoparticle solution was diluted to different concentrations and each solution was characterized. The concentration of each nanoparticle solution was expressed by the pluronic concentration. For example, we selected $ADP(OH)_2$-Bottom in 5% F98 nanoparticle as the original sample and diluted it by 5, 25, and 125 times correspondingly. Thus, we obtained $ADP(OH)_2$-Bottom in 1%, 0.2% and 0.04% F98 nanoparticle, respectively. The characterization of all the nanoparticles in the section were summarized in *Table 4*. *Figure 5A* shows their normalized fluorescence intensity as a function of temperature. Their T_{th}s were ~28, 34, 37, and 41 ℃, respectively. The result indicates that when the nanoparticles were diluted to a lower concentration, the Tth shifted to the higher temperature. *Figure 5B,C,D* respectively show the similar measurement results of the other three nanoparticle samples: $ADP(OH)_2$-Bottom in F127 nanoparticle, $ADP(OH)_2$-Top in F68 nanoparticle, and ZnttbPc in F98 nanoparticle. When each sample was diluted to a lower concentration, its T_{th}s increased correspondingly. Thus, we concluded that the nanoparticle's T_{th}s increased with the decrease of the concentration for the adopted fluorophores and pluronics.

Observation of different temperature-switching thresholds of nanoparticles under a camera

We respectively injected four nanoparticle samples with different temperature thresholds into four silicone tubes and merged tubes into a water bath whose temperature was controlled via the same method discussed before. The dynamic fluorescence change of the samples *vs*. temperature was simultaneously monitored via a camera. The silicone tubes have an inner diameter of 760 μm. A 671 nm laser was adopted as the excitation light. An intensified charge-coupled device (ICCD) camera was placed on the top for fluorescence imaging of the four tubes. Four 830 nm long-pass interference filters and one 830 nm long-pass absorption filter were placed in front of the camera lens as emission filters. The water temperature was increased gradually from room temperature =22 ℃ to a high temperature =50 ℃. At different temperatures (step size: 1 ℃), the ICCD camera recorded the fluorescence image of all the tubes. As an example, we imaged the samples of $ADP(OH)_2$-Bottom encapsulated in pluronic F98 with a concentration of 5%, 1%, 0.2% and 0.04%, which correspond to different temperature thresholds. *Figure 6A* shows a white image of the four tubes under the camera. From the bottom to top, the sample concentration is 5%, 1%, 0.2% and 0.04%. *Figure 6B* shows the normalized background fluorescence image of the tubes at room temperature =22 ℃ when all the four nanoparticles are at their off states. Due to the dilution, the background fluorescence decreases with the reduction of the nanoparticle concentration. Note that the tube at the bottom has the highest nanoparticle concentration and therefore it shows the most obvious background signal. Background fluorescence signal is usually caused by a fact that the fluorophores in the nanoparticles are not

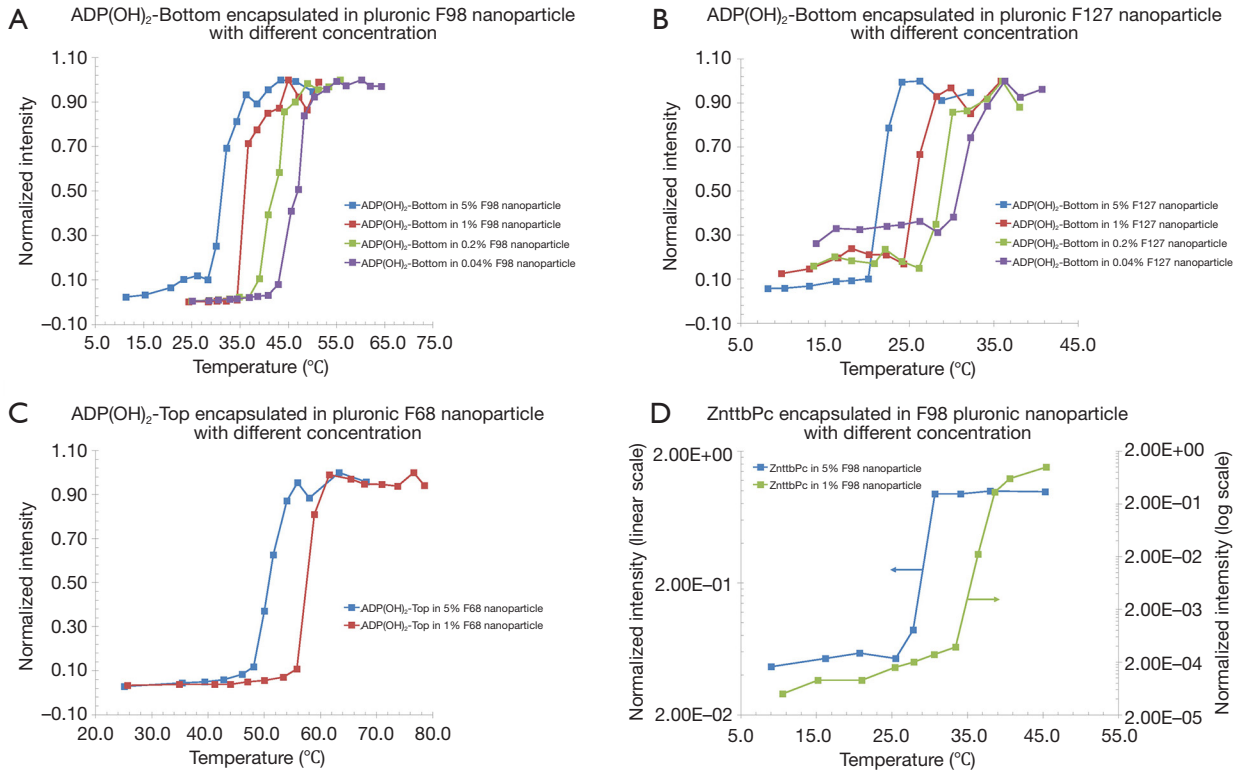

Figure 5 Fluorescence intensity as a function of temperature of (A) $ADP(OH)_2$-Bottom encapsulated in 5% pluronic F98, diluted to 1% pluronic F98, diluted to 0.2% pluronic F98, and diluted 0.04% pluronic F98 nanoparticle; (B) $ADP(OH)_2$-Bottom encapsulated in 5% pluronic F127, diluted 1% pluronic F127, diluted to 0.2% pluronic F127, and diluted to 0.04% pluronic F127 nanoparticle; (C) $ADP(OH)_2$-Top encapsulated in 5% pluronic F68, and diluted to 1% pluronic F68 nanoparticle; and (D) ZnttbPc encapsulated in 5% pluronic F98, and diluted to 1% pluronic F98 nanoparticle.

completely switched off even though they are at off states. Usually, we call this background signal as non-100%-off background signal. In order to visualize the four tubes in the same figure, we individually normalized the fluorescence signal for each tube. *Figure 6C* show the corresponding results. The images show their fluorescence intensities at the temperatures of 22, 29, 31, 38, 42 and 48 ℃, respectively. A displaying threshold of 0.25 was applied for each image so that the background fluorescence can be removed. Clearly, when the temperature was 22 and 29 ℃ (*Figure 6C1*,*C2*), all the fluorescence tubes were at "off" state, which indicated that the two temperatures were below the T_{th}s of all samples. When the temperature rose to 31 ℃ (*Figure 6C3*), the first bottom tube [filled with $ADP(OH)_2$-Bottom encapsulated in 5% pluronic F98 nanoparticles] was switched "on". When the temperature was 38 ℃ (*Figure 6C4*), the second bottom tube [filled with $ADP(OH)_2$-Bottom encapsulated in 1% pluronic F98 nanoparticles] was switched "on". When the temperature was 42 ℃ (*Figure 6C5*), the third bottom tube [filled with $ADP(OH)_2$-Bottom encapsulated in 0.2% pluronic F98 nanoparticles] was switched "on". Finally, when the temperature rose to 48 ℃ (*Figure 6C6*), all the tubes were switched "on". *Figure 6D* shows the normalized fluorescence intensity in each tube plotted as a function of temperature. The measurement results were similar to that in *Figure 5A*. This experiment clearly shows that the measured T_{th}s of nanoparticles in our previous system (6) is reliable and also repeatable under the camera-based fluorescence imaging system.

Discussion

The nanoparticles are appropriate for ultrasound-switchable fluorescence (USF) imaging

Some pluronic nanoparticles have been selected and adopted as USF contrast agents in our previous work

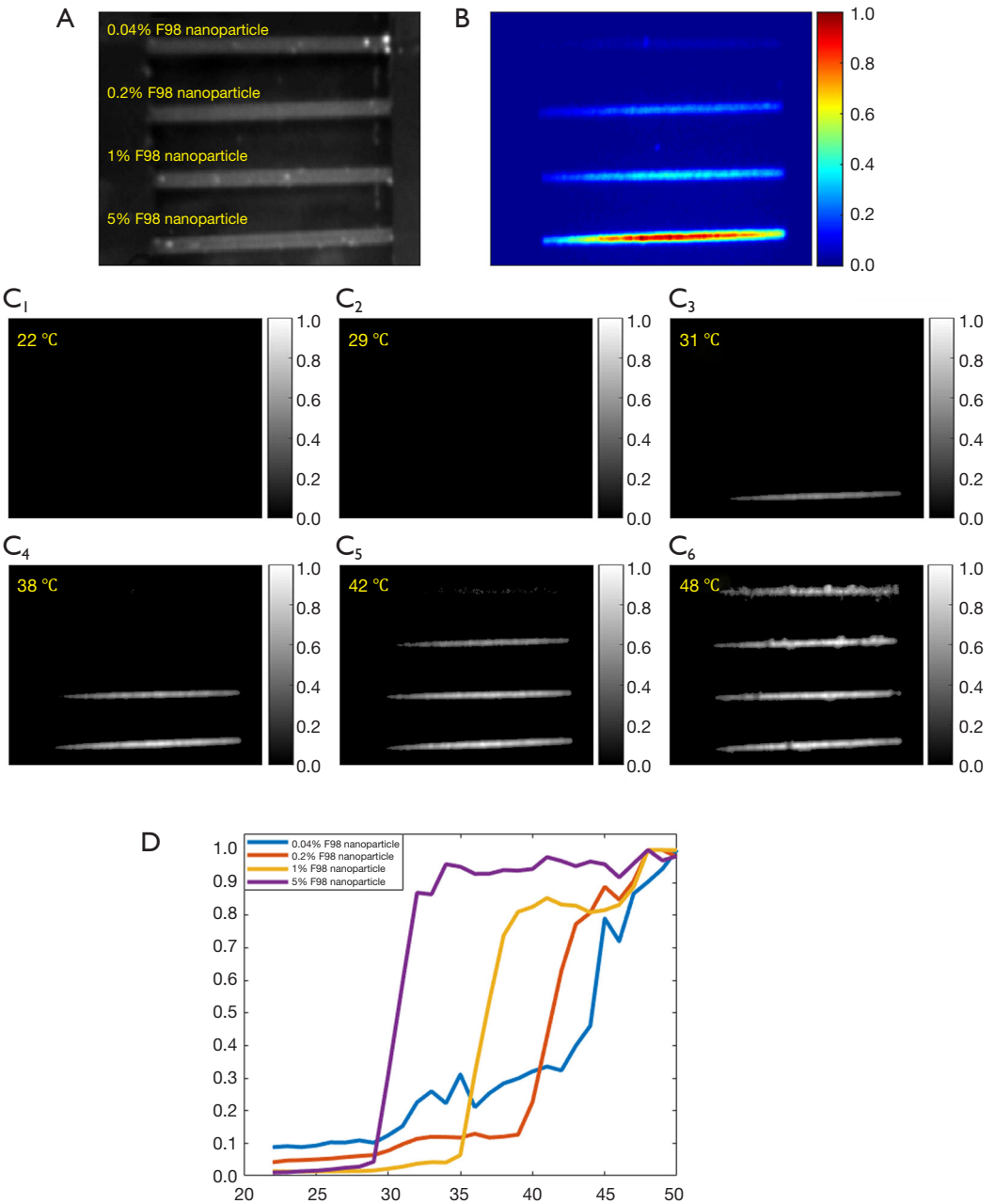

Figure 6 (A) A white image of the four silicone tubes. Each tube, from bottom to top, was filled with ADP(OH)$_2$-Bottom encapsulated in 5% pluronic F98, diluted to 1% pluronic F98, diluted to 0.2% pluronic F98, and diluted 0.04% pluronic F98 nanoparticle, correspondingly. (B) Normalized fluorescence image of the four silicone tube when the temperature = 22 °C. (C: 1-6) Each tube was switched "on" one after another with the increase of temperature. Note that in each tube its fluorescence intensity was normalized as a function of temperature. A displaying threshold =0.25 was applied in each image for visualization of either the fluorescence was still "off" or already switched "on". (D) Normalized fluorescence intensity in each tube plotted as a function of temperature.

(8,15-17). They have several advantages in USF imaging. First, the fluorophores (i.e., ADP or ZnPC series) are NIR dyes so their fluorescence can penetrate deeper biological tissue compared with light with visible wavelengths. Second, compared with other USF contrast agents, many nanoparticles (i.e., ADP in 5% F98 nanoparticle) show a high I_{on}/I_{off}, which helps quench the background fluorescence to reduce background noise and further improve signal-to-noise ratio (SNR) in USF image. Third, some nanoparticles (i.e., ZnttbPc in 5% F98 nanoparticle) also showed a high τ_{on}/τ_{off}. A high τ_{on}/τ_{off} could help increase the SNR of a USF image when using a time-domain USF imaging system (20). In conclusion, the nanoparticles have excellent thermal-switchable properties and are appropriate contrast agents for USF imaging.

The nanoparticles are appropriate for temperature sensing

In this work, we demonstrated that the nanoparticles' T_{th}s varied in a wide temperature range from ~20 to ~64 ℃. Their T_{th}s could be adjusted by changing the pluronic categories and/or the nanoparticle concentrations. These nanoparticles usually had an excellent fluorescence intensity switching property (i.e., a high I_{on}/I_{off}) so that they should have very high temperature sensitivity. Also, these nanoparticles had a TBW of a few to tens of Celsius degrees (from 3 up to 20 ℃). Thus, the nanoparticles can be used as temperature sensors. Their temperature sensing ranges depend on the TBW: when the temperature crosses the TBW, the fluorescence increases significantly. For example, the ADP in 5% F98 nanoparticle has a fluorescence intensity increase most when the temperature rises from ~28 to ~34 ℃ (seen in *Figure 2A*), which means this nanoparticle has the most efficient temperature sensing range from 28 to 34 ℃. By combining these nanoparticles with different T_{th}s and TBWs, we can develop temperature sensors covering a wide temperature range. Further work about this application will be explored in our future work.

Conclusions

In this work, we successfully synthesized, characterized, and selected a series of NIR nanoparticles, by encapsulating two series of NIR fluorophores (ADP and ZnPc) in four pluronic polymers (F127, F98, F68, and F38). These nanoparticles showed excellent temperature-switchable properties of fluorescence intensity and/or lifetime. Also, we investigated some factors (i.e., pluronic categories and nanoparticles' concentration) that significantly affected the nanoparticles' T_{th}s while other (i.e., fluorophore categories) that weakly affected T_{th}s. By selecting appropriate pluronic categories and adjusting the nanoparticle's concentration, we can synthesize the nanoparticles with a wide range of T_{th}s. These temperature-switchable fluorescence nanoparticles can be used for biomedical imaging (such as tissue fluorescence and/or USF imaging) and *in vivo* tissue temperature sensing/imaging.

Acknowledgments

Thanks for Dr. Kytai Nguyen and Dr. Yi Hong for allowing us to use some equipment in their labs to synthesize and characterize contrast agents. Thanks for Dr. Francis D'Souza for providing the ADP series fluorophores.

Funding: This work was supported in part by funding from Cancer Prevention & Research Institute of Texas (CPRIT) RP170564 (Baohong Yuan).

Footnote

Provenance and Peer Review: With the arrangement by the Guest Editors and the editorial office, this article has been reviewed by external peers.

Conflicts of Interest: All authors have completed the ICMJE uniform disclosure form (available at http://dx.doi.org/10.21037/qims-20-797). The special issue "Advanced Optical Imaging in Biomedicine" was commissioned by the editorial office without any funding or sponsorship. SY reports grants from Cancer Prevention & Research Institute of Texas, during the conduct of the study; in addition, Dr. SY has a patent Systems and Methods for Thermometry and Theranostic Applications pending. ZW reports grants from Cancer Prevention & Research Institute of Texas, during the conduct of the study. TY reports grants from Cancer Prevention & Research Institute of Texas, during the conduct of the study; in addition, Dr. TY has a patent Systems and Methods for Thermometry and Theranostic Applications pending, a patent Ultrasound-switchable fluorescence imaging having improved imaging speed pending, and a patent Significantly improving sensitivity of ultrasound-switchable fluorescence technique for high-resolution, deep tissue, and dynamic imaging pending. BY reports grants from Cancer Prevention & Research Institute of Texas , during the conduct of the study; in addition, Dr. BY has a patent Systems and Methods for high-

resolution imaging issued, a patent Systems and Methods for Thermometry and Theranostic Applications pending, a patent Highly specific tissue imaging pending, a patent Multiple biomarkers imaging for high specificity pending, a patent Ultrasound-switchable fluorescence imaging having improved imaging speed pending, a patent Systems and Methods for surgical guidance in breast cancer surgery and lymph node dissection pending.

References

1. Frangioni JV. In vivo near-infrared fluorescence imaging. Curr Opin Chem Biol 2003;7:626-34.
2. Hong G, Antaris AL, Dai H. Near-infrared fluorophores for biomedical imaging. Nat Biomed Eng 2017;1:0010.
3. Terai T, Nagano T. Fluorescent probes for bioimaging applications. Curr Opin Chem Biol 2008;12:515-21.
4. Kobayashi H, Ogawa M, Alford R, Choyke PL, Urano Y. New strategies for fluorescent probe design in medical diagnostic imaging. Chem Rev 2010;110:2620-40.
5. Guo Z, Park S, Yoon J, Shin I. Recent progress in the development of near-infrared fluorescent probes for bioimaging applications. Chem Soc Rev 2014;43:16-29.
6. Cheng B, Wei MY, Liu Y, Pitta H, Xie Z, Hong Y, Nguyen KT, Yuan B. Development of Ultrasound-switchable Fluorescence Imaging Contrast Agents based on Thermosensitive Polymers and Nanoparticles. IEEE J Sel Top Quantum Electron 2014;20:6801214.
7. Yu S, Cheng B, Yao T, Xu C, Nguyen KT, Hong Y, Yuan B. New generation ICG-based contrast agents for ultrasound-switchable fluorescence imaging. Sci Rep 2016;6:35942.
8. Cheng B, Bandi V, Yu S, D'Souza F, Nguyen KT, Hong Y, Tang L, Yuan B. The Mechanisms and Biomedical Applications of an NIR BODIPY-Based Switchable Fluorescent Probe. Int J Mol Sci 2017;18:384.
9. Saremi B, Bandi V, Kazemi S, Hong Y, D'Souza F, Yuan B. Exploring NIR Aza-BODIPY-Based Polarity Sensitive Probes with ON-and-OFF Fluorescence Switching in Pluronic Nanoparticles. Polymers (Basel) 2020;12:540.
10. Cui J, Kwon JE, Kim HJ, Whang DR, Park SY. Smart Fluorescent Nanoparticles in Water Showing Temperature-Dependent Ratiometric Fluorescence Color Change. ACS Appl Mater Interfaces 2017;9:2883-90.
11. Zhao Y, Shi C, Yang X, Shen B, Sun Y, Chen Y, Xu X, Sun H, Yu K, Yang B, Lin Q. pH- and Temperature-Sensitive Hydrogel Nanoparticles with Dual Photoluminescence for Bioprobes. ACS Nano 2016;10:5856-63.
12. Cheng CC, Liao ZS, Huang JJ, Lee DJ, Chen JL. Supramolecular polymer micelles as universal tools for constructing high-performance fluorescent nanoparticles. Dyes and Pigments 2017;137:284-292.
13. Kakade S, Ghosh R, Palit DK. Excited State Dynamics of Zinc–Phthalocyanine Nanoaggregates in Strong Hydrogen Bonding Solvents. J Phys Chem C 2012;116:15155-66.
14. Gümrükçü G, Karaoğlan GK, Erdoğmuş A, Gül A, Avcıata U. Photophysical, photochemical, and BQ quenching properties of zinc phthalocyanines with fused or interrupted extended conjugation. J Chem 2014;2014:435834.
15. Cheng B, Bandi V, Wei MY, Pei Y, D'Souza F, Nguyen KT, Hong Y, Yuan B. High-Resolution Ultrasound-Switchable Fluorescence Imaging in Centimeter-Deep Tissue Phantoms with High Signal-To-Noise Ratio and High Sensitivity via Novel Contrast Agents. PLoS One 2016;11:e0165963.
16. Kandukuri J, Yu S, Cheng B, Bandi V, D'Souza F, Nguyen KT, Hong Y, Yuan B. A Dual-Modality System for Both Multi-Color Ultrasound-Switchable Fluorescence and Ultrasound Imaging. Int J Mol Sci 2017;18:323.
17. Kandukuri J, Yu S, Yao T, Yuan B. Modulation of ultrasound-switchable fluorescence for improving signal-to-noise ratio. J Biomed Opt 2017;22:76021.
18. Yao T, Yu S, Liu Y, Yuan B. Ultrasound-Switchable Fluorescence Imaging via an EMCCD Camera and a Z-Scan Method. IEEE J Sel Top Quantum Electron 2019;25:7102108.
19. Yao T, Yu S, Liu Y, Yuan B. In vivo ultrasound-switchable fluorescence imaging. Sci Rep 2019;9:9855.
20. Yu S, Yao T, Yuan B. An ICCD camera-based time-domain ultrasound-switchable fluorescence imaging system. Sci Rep 2019;9:10552.
21. Liu Y, Yao T, Cai W, Yu S, Hong Y, Nguyen KT, Yuan B. A Biocompatible and Near-Infrared Liposome for In Vivo Ultrasound-Switchable Fluorescence Imaging. Adv Healthc Mater 2020;9:e1901457.
22. Yu S, Yao T, Liu Y, Yuan B. In vivo ultrasound-switchable

fluorescence imaging using a camera-based system. Biomed Opt Express 2020;11:1517-38.
23. Pandey N, Menon JU, Takahashi M, Hsieh JT, Yang J, Nguyen KT, Wadajkar AS. Thermo-responsive Fluorescent Nanoparticles for Multimodal Imaging and Treatment of Cancers. Nanotheranostics 2020;4:1-13.
24. Wang Z, Yong TY, Wan J, Li ZH, Zhao H, Zhao Y, Gan L, Yang XL, Xu HB, Zhang C. Temperature-sensitive fluorescent organic nanoparticles with aggregation-induced emission for long-term cellular tracing. ACS Appl Mater Interfaces 2015;7:3420-5.
25. Julià López A, Ruiz-Molina D, Landfester K, Bannwarth MB, Roscini C. Off/On Fluorescent Nanoparticles for Tunable High-Temperature Threshold Sensing. Adv Funct Mater 2018;28:1801492.
26. Amin AN, El-Khouly ME, Subbaiyan NK, Zandler ME, Supur M, Fukuzumi S, D'Souza F. Syntheses, electrochemistry, and photodynamics of ferrocene-azadipyrromethane donor--acceptor dyads and triads. J Phys Chem A 2011;115:9810-9.
27. Bandi V, El-Khouly ME, Ohkubo K, Nesterov VN, Zandler ME, Fukuzumi S, D'Souza F. Excitation-wavelength-dependent, ultrafast photoinduced electron transfer in bisferrocene/BF2-chelated-azadipyrromethene/fullerene tetrads. Chemistry 2013;19:7221-30.
28. Bandi V, El-Khouly ME, Nesterov VN, Karr PA, Fukuzumi S, D'Souza F. Self-assembled via metal–ligand coordination azaBODIPY–zinc phthalocyanine and azaBODIPY–zinc naphthalocyanine conjugates: synthesis, structure, and photoinduced electron transfer. J Phys Chem C 2013;117:5638-49.
29. Zinc phthalocyanine, Dye content 97%. Available online: https://pubchem.ncbi.nlm.nih.gov/substance/24860701

Cite this article as: Yu S, Wang Z, Yao T, Yuan B. Near-infrared temperature-switchable fluorescence nanoparticles. Quant Imaging Med Surg 2021;11(3):1010-1022. doi: 10.21037/qims-20-797

